Electrochemical Epitaxial Growth of a Pt(111) Phase on an Au(111) Electrode

Kohei Uosaki,* Shen Ye, Hideo Naohara, Yasuhiro Oda, Toshio Haba, and Toshihiro Kondo

Physical Chemistry Laboratory, Division of Chemistry, Graduate School of Science, Hokkaido University, Sapporo 060, Japan

Received: May 29, 1997; In Final Form: July 10, 1997[⊗]

The electrochemical deposition of platinum on an Au(111) single-crystal electrode in acidic solutions containing H_2PtCl_6 was studied using an electrochemical scanning tunneling microscope (STM) and electrochemical quartz crystal microbalance (EQCM). The STM investigation showed an ordered adlayer of $PtCl_6^{2-}$ on the electrode surface during the electrochemical deposition of platinum and a Pt(111)-(1×1) structure on the electrode surface after the electrode was rinsed with a Pt complex-free solution. Formations of the Pt(111) bulk phase and surface structure of Pt(111)-(1×1) were confirmed by X-ray diffraction (XRD) and the underpotential deposition of copper and hydrogen, respectively.

Introduction

Electrochemical deposition of foreign metals on metal and semiconductor substrates is not only technologically important but also of fundamental significance because many interesting elementary steps such as electron transfer, desolvation, phase change, nucleation, and crystal growth are involved in this process. To understand and control the electrochemical deposition process, it is essential to monitor the surface structure *in situ* with atomic/molecular resolution. It is particularly interesting to investigate the surface structure of the electrode during metal deposition when metal complexes are used as a reactant. Although many reports are available for the *in situ* observation of so-called underpotentially deposited (UPD) metal layers such as copper,[1−4] silver,[5−9] and lead,[10] the investigation of the electrochemical deposition process on an atomic level is rather limited and no evidence has been given for the adsorption of the reactant, i.e., metal ions, on the electrode surface during the electrochemical deposition.

The establishment of the preparation method of smooth thin layers of noble metals with good mechanical strength is essential in order to effectively utilize the limited resources of the noble metal elements. Platinum is one of the most important catalysts for many chemical reactions,[11,12] and the electrocatalytic properties of metal electrodes are often improved by the deposition of a small amount of platinum on the surface.[13−15] Thus, it is very important to deposit platinum in a controlled manner. The first layer-by-layer growth of platinum on Pt(111) was achieved by molecular-beam epitaxy in a ultrahigh vacuum (UHV).[16] Recently, platinum was epitaxially grown on the basal-plane (0001) surface of a sapphire crystal at 600 °C by means of ion-beam sputtering.[17,18] The combination of electrochemical deposition of platinum on a Pt polycrystalline electrode from H_2PtCl_6 solution and heat treatment was reported to give the Pt(100) phase.[19,20] Although electrochemical deposition is more convenient and economical than the growth in UHV and the electrochemical deposition of platinum has been very extensively studied, [21−27] observation and control of the electrochemical deposition of platinum on other metal substrates at an atomic level are not available yet.

In this paper, the electrochemical deposition of platinum on an Au(111) single-crystal electrode in acidic solutions containing H_2PtCl_6 was investigated using an electrochemical scanning tunneling microscope (STM) and electrochemical quartz crystal microbalance (EQCM). An ordered adlayer of $PtCl_6^{2-}$ was observed on the electrode surface by an *in situ* STM during the electrochemical deposition of platinum. This structure disappeared and the Pt(111)-(1×1) structure was observed on the electrode surface after the electrode was rinsed with a H_2PtCl_6-free solution, suggesting that the adsorption of the $PtCl_6^{2-}$ complex was weak. Formations of the Pt(111) bulk phase and surface structure of Pt(111)-(1×1) were confirmed by X-ray diffraction (XRD) measurement and the underpotential deposition of copper and hydrogen, respectively.

Experimental Section

STM observations were carried out on an atomically flat (111) facet formed on the surface of a gold single-crystal bead which was prepared using Clavilier's method.[28] Electrochemical characterizations were carried out on Au(111) and Pt(111) single-crystal electrodes which were prepared using Clavilier's method,[28] cut, and mechanically polished. EQCM and XPS/XRD measurements were carried out at gold electrodes prepared by vacuum evaporation of 3 nm titanium followed by 150 nm gold onto a 5 MHz AT-cut quartz crystal plate (diameter 13 mm) and slide glass, respectively, at 300 °C with an evaporation rate of 0.01 nm/s. A standard surface treatment procedure including annealing with a gas/O_2 flame and quenching in pure water was used to obtain reproducible surface states of all the substrates.[28] The formation of the highly ordered Au(111) phase with a long-range terrace-step structure by these procedures on various substrates has been well documented[29,30] and was confirmed in this study.

Electrolyte solutions were prepared using Suprapure grade $HClO_4$ (Wako Pure Chemicals), H_2SO_4 (Wako Pure Chemicals), $H_2PtCl_6 \cdot H_2O$ (Kanto Chemicals), and Milli-Q water. The concentration of the platinum complex in solution was adjusted by adding 3 mM H_2PtCl_6 stock solution into 50 mM $HClO_4$ or 50 mM H_2SO_4 solution.

STM measurements were carried out by using a NanoScope E (Digital Instrument) in the ECSTM mode with a homemade electrochemical STM cell which can accommodate a single-crystal bead electrode. STM images were usually obtained in constant current mode unless otherwise stated. A small quasi-reversible hydrogen electrode and a platinum wire (diameter 0.3 mm) were used as a reference and a counter electrode,

* Corresponding author: Tel +81-11-706-3812; Fax +81-11-706-3440; E-mail uosaki@pcl.chem.hokudai.ac.jp.

[⊗] Abstract published in *Advance ACS Abstracts,* August 15, 1997.

S1089-5647(97)01740-9 CCC: $14.00

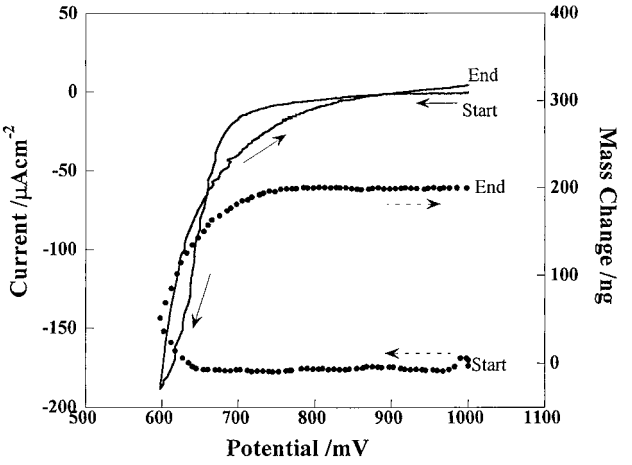

Figure 1. Potential dependence of current (solid line) and the mass change (dotted line) at a gold/EQCM electrode in a solution containing 50 mM $HClO_4$ and 0.6 mM H_2PtCl_6. Sweep rate: 20 mV/s.

respectively. STM tips were simply cut Pt wire (0.3 mm) insulated with nail polish.

For the electrochemical and EQCM measurements, the electrode potential was controlled by a potentiostat (Hokuto Denko, HA-151), and external potential modulation was provided by a function generator (Hokuto Denko, HB-111). A quasi-reversible hydrogen electrode and a platinum wire (diameter 0.5 mm) were used as the reference and counter electrode, respectively. All the potentials in this paper are presented with respect to the reversible hydrogen electrode (RHE).

The resonant frequency of the quartz crystal electrode, which was oscillated by a homemade oscillation circuit, was simultaneously monitored for electrode potential and current by a frequency counter (Hewlett Packard, HP53131A) controlled by a personal computer (NEC PC9821cb2) through a GPIB interface. The frequency stability of the EQCM system was better than 0.1 Hz for a sampling gate time of 0.1 s. Details of the EQCM system used in this study were similar to those previously described.[31] The mass change was estimated from the resonant frequency change using the Sauerbrey equation.[32,33] The mass sensitivity of the 5 MHz AT-cut quartz crystal was calibrated[34] by the deposition reactions of silver and lead and was -19.3 ng/(Hz cm^2).

XPS measurements were carried out using a XPS-700 spectrometer (RIGAKU) with an incidence angle of 80°. The spectra were recorded using Mg Kα X-rays with an energy of 1253.6 eV. The acceleration voltage and emission current used for generating the X-rays were 10 kV and 30 mA. XRD measurements were carried out using an RINT-2200 (RIGAKU) with a four-circle diffractometer. Samples for the XPS and XRD measurements were removed from the electrolyte solution under potential control, then rinsed with Milli-Q water, and finally dried with purified nitrogen.

All the measurements were carried out after the solution was deaerated by passing purified N_2 gas for at least 20 min through the solution.

Results and Discussion

EQCM Investigation of Platinum Deposition on an Au(111) Electrode. Figure 1 shows the potential dependence of the current and the mass change at a gold/EQCM electrode for the first potential cycle between +1.0 and +0.6 V in 50 mM $HClO_4$ solution after H_2PtCl_6 solution was added at +1.0 V (H_2PtCl_6 concentration 0.6 mM). A cathodic current (solid line) started to flow around +0.80 V and quickly increased as the potential became more negative than +0.70 V. The surface mass (dotted line) significantly increased when the potential became more negative than +0.65 V. Even after the sweep direction was reversed at +0.6 V, a cathodic current flowed and the surface mass continued to increase until the potential became +0.80 V. The cathodic current and the mass increase suggested that the platinum deposition took place in this potential region. This is reasonable as the standard redox potential of $PtCl_6^{2-}$/Pt is 0.70 V vs RHE.[21]

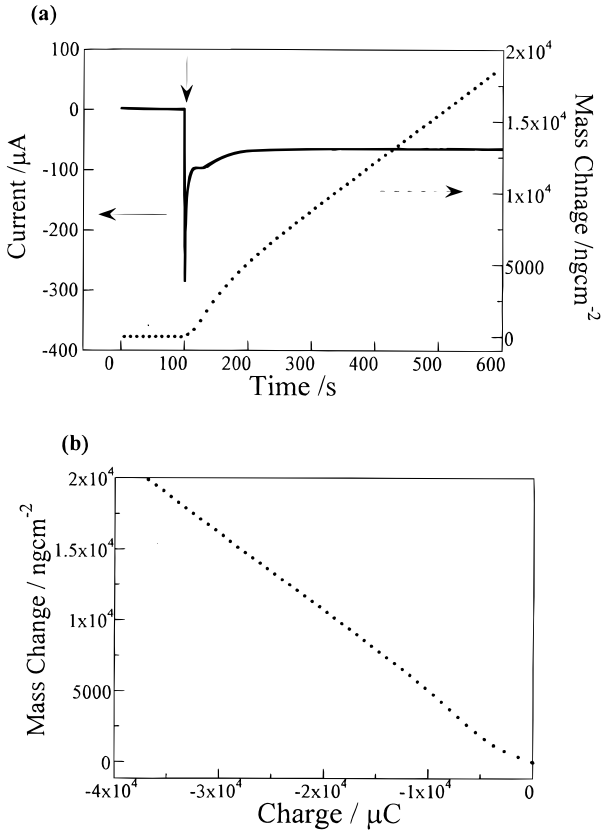

Figure 2. (a) Time dependence of current (solid line) and the mass change (dotted line) at a gold/EQCM electrode in a solution containing 50 mM $HClO_4$ and 0.6 mM H_2PtCl_6 when the potential was stepped from +1.0 to +0.60 V, as shown by the arrow. (b) Relationship between the mass change and electric charge after the potential was stepped from +1.0 to +0.60 V, shown in part a.

In order to analyze this deposition process more quantitatively, the time dependence of the current and the mass change were simultaneously recorded when the potential was stepped from +1.0 to +0.60 V. An almost constant cathodic current flow and the surface mass increase of constant rate were observed after the potential step (Figure 2a). A good linear relationship was obtained between the mass change and the cathodic charge, as shown in Figure 2b, and the mass change per mole electron, abbreviated as *mpe*, was estimated from the slope of the straight line as 48.5 g/(mol electron). This value is in good agreement with the calculated value for a four-electron reduction process ($PtCl_6^{2-} + 4e^- \rightarrow Pt + 6Cl^-$), 48.77 (=195.08/4) g/(mol electron).

***In Situ* Electrochemical STM Observation during the Platinum Deposition.** Electrochemical deposition of platinum on an Au(111) electrode was monitored by an *in situ* electrochemical STM in acidic solutions containing H_2PtCl_6. Figure 3 shows STM images (current image in constant height mode) of the Au(111) electrode surface (40 × 40 nm^2) recorded (a) at +0.95 V and (b) 10 min and (c) 30 min, respectively, after the potential was stepped from +0.95 to +0.70 V in a solution containing 50 mM H_2SO_4 and 0.05 mM H_2PtCl_6. The deposi-

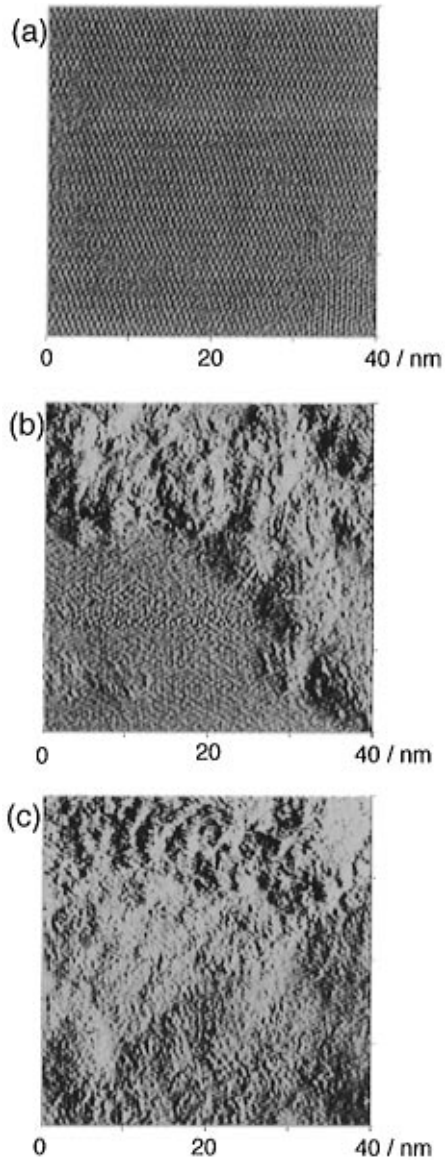

Figure 3. STM images (40 × 40 nm^2 region) of platinum deposition process on an Au(111) substrate (a) at +0.95 V and (b) 10 min and (c) 30 min, respectively, after the potential was stepped from +0.95 to +0.70 V in a solution containing 50 mM H_2SO_4 and 0.05 mM H_2PtCl_6.

tion rate of platinum was kept low by using a low H_2PtCl_6 concentration (0.05 mM) and small overpotential (+0.70 V).

An STM image obtained at +0.95 V where neither a cathodic nor anodic current flowed (Figure 3a) showed an ordered adlayer structure. The spots with the same brightness showed a hexagonal symmetry with a nearest neighbor distance of ca. 0.76 nm. This adlayer structure is exactly the same as that of the $PtCl_6^{2-}$ adlayer on Au(111) observed in 50 mM $HClO_4$ + 0.6 mM H_2PtCl_6 solution, i.e., Au(111)-$\sqrt{7}\times\sqrt{7}R19.1°$.[34] Thus, the $PtCl_6^{2-}$ complex formed an adlayer of the same structure on the Au(111) surface in both $HClO_4$ and H_2SO_4 solutions.

As soon as the potential was stepped to +0.70 V, the deposition of the platinum layer of monoatomic height was initiated. The growth of this layer seemed to be essentially two-dimensional, at least during the initial stage, as clearly seen in Figure 3b,c. The deposited platinum layer grew from the top right-hand portion of the image (Figure 3b) and covered the entire area of the image after prolonged deposition (Figure 3c). The bottom left-hand portion of Figure 3b is the Au(111) covered with a $PtCl_6^{2-}$ adlayer of $\sqrt{7}\times\sqrt{7}R19.1°$ structure (cf. Figure 3a). Although the image is noisier on the platinum layer of Figure 3, the images obtained in the constant current mode showed that the height of this layer was monoatomic. A noisier image may reflect the fact that the reduction of $PtCl_6^{2-}$ and/or diffusion of platinum atoms are taking place on the deposited layer. The terrace size of the platinum layer seemed to be much smaller than that of the Au(111) surface before the platinum deposition. A number of small clusters were also observed on the platinum layer (Figures 3b,c). These clusters are higher than the first platinum layer by a monoatomic height of the platinum layer. This means the growth of the platinum layer is not a perfect two-dimensional growth. One reason why perfect two-dimensional growth was not achieved is the slower surface diffusion rate of platinum atoms, i.e., slower lateral growth rate because platinum shows a much smaller self-diffusion coefficient at room temperature than those of other metal elements, such as lead, silver, and copper.[35,36]

Similar STM images were obtained during the platinum deposition on an Au(111) electrode in 50 mM $HClO_4$ solution with the same concentration of H_2PtCl_6.

Although an atomically resolved structure was not obtained on top of the platinum layer in Figure 3, the higher resolution image showed an ordered structure even on the platinum layer. Figure 4a shows a high-resolution STM image (5 × 5 nm^2) obtained at +0.70 V in a solution containing 50 mM $HClO_4$ and 0.6 mM H_2PtCl_6 on top of the platinum-grown layer. A rather complicated adlayer structure with different brightness and contrast was observed. The spots with the same brightness showed a hexagonal symmetry with a nearest neighbor distance of ca. 0.76 nm. The nearest neighbor distance between the brightest spot and the second brightest spot was ca. 0.33 nm. This adlayer structure is very similar to that of $PtCl_6^{2-}$ adsorbed on Au(111) as a $\sqrt{7}\times\sqrt{7}R19.1°$ adlattice.[34]

After the STM image shown in Figure 4a was obtained, the solution in the STM cell was replaced by 50 mM $HClO_4$ several times while the potential was held at +0.70 V so that the electrode was thoroughly rinsed. Figure 4b shows the STM image (5 × 5 nm^2 region) of the surface of the same electrode in a solution containing only 50 mM $HClO_4$ after the rinse treatment. The adlattice structure observed in Figure 4a disappeared, and the highly ordered surface structure of a hexagonal array with a neighbor atomic distance of 0.28 nm was observed. This distance is very close to that of the unit lattice of the Pt(111) or Au(111) surface. Since the neighbor atomic distances of Pt(111) (0.278 nm) and Au(111) (0.288 nm) are similar, it is difficult to determine whether the surface was Pt(111) or Au(111) by the STM measurement only. XPS measurements were carried out to confirm the existence of platinum on the Au(111) surface after these treatments. While a prominent peak at 84.1 eV and a small peak at 75.6 eV attributed to Au $4f_{7/2}$ and Au $5p_{3/2}$, respectively, were observed in the XP spectrum of the bare gold electrode,[37] these peaks became significantly small and two new peaks were observed at 74.5 and 71.2 eV at the gold electrode which was kept at +0.70 V for 1 min in a solution containing 50 mM $HClO_4$ and 0.6 mM H_2PtCl_6 and rinsed by Milli-Q water before the XPS measurement. These two peaks were assigned to Pt $4f_{7/2}$ and Pt $4f_{5/2}$, respectively.[37] These results clearly showed that the surface is platinum, and therefore, the image shown in Figure 4b should correspond to the Pt(111)-(1×1) structure formed on the Au(111) substrate.

The fact that the adlayer structure disappeared after the electrode was rinsed showed that $PtCl_6^{2-}$ was weakly adsorbed on the Pt(111) surface. We have already reported that it

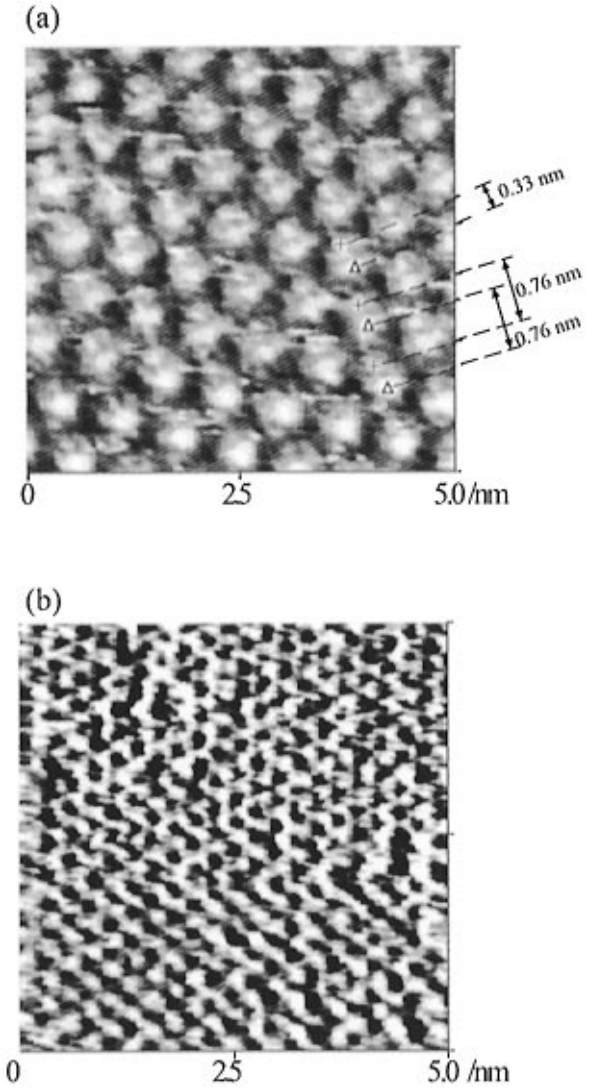

Figure 4. High-resolution STM images (5×5 nm^2 region) of (a) an Au(111) electrode obtained at +0.70 V in a solution containing 50 mM $HClO_4$ and 0.6 mM H_2PtCl_6 and (b) the same electrode in 50 mM $HClO_4$ after the solution in the STM cell was replaced several times by 50 mM $HClO_4$ while the potential was held at +0.70 V after the STM image (a) was obtained. Note the imaged portion was not the same.

adsorbed weakly on the Au(111) surface. The adlayer structure of the $PtCl_6^{2-}$ on the Pt(111) surface can be well explained by the model shown in Figure 5, i.e., Pt(111)-$\sqrt{7}\times\sqrt{7}R19.1°$, which is essentially the same as that of the $PtCl_6^{2-}$ adlayer structure on the Au(111) surface.[34]

XRD Measurement of the Platinum Deposit. To confirm the formation of the Pt(111) phase on the Au(111) substrate, XRD measurements were carried out. Figure 6 shows the XRD patterns of (a) a gold electrode evaporated on a glass slide at 300 °C (Au/glass slide), (b) a gold electrode evaporated on a glass slide at 300 °C on which platinum was electrochemically deposited at 0.05 V for 45 min (ca. 250 Pt layers) in a solution containing 50 mM H_2SO_4 and 1 mM H_2PtCl_6 (Pt/Au/glass slide), and (c) a bare polycrystalline Pt disk. The assignments based on the JCPDS data were given for respective reflection peaks in the figure.[38] Only Au(111) and Au(222) reflections were observed for the Au/glass slide as shown in Figure 6a. This confirms that a well-defined Au(111) phase was formed on the glass slide under this condition.[30] The XRD patterns of the Pt/Au/glass slide (Figure 6b) show the (111) and (222) peaks of platinum in addition to the (111) and (222) peaks of gold.

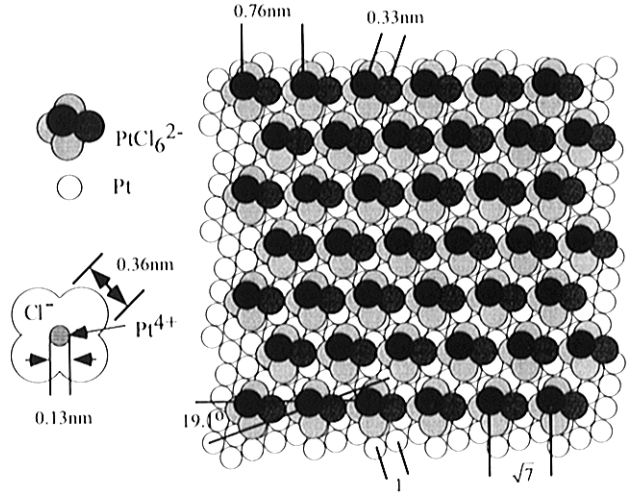

Figure 5. Model for the adlayer structure of $PtCl_6^{2-}$ species adsorbed on a Pt(111) phase which is electrochemically deposited on an Au(111) substrate with a lattice structure of $\sqrt{7}\times\sqrt{7}R19.1°$. A molecule model drawn from its respective atom−atom distance is also shown.

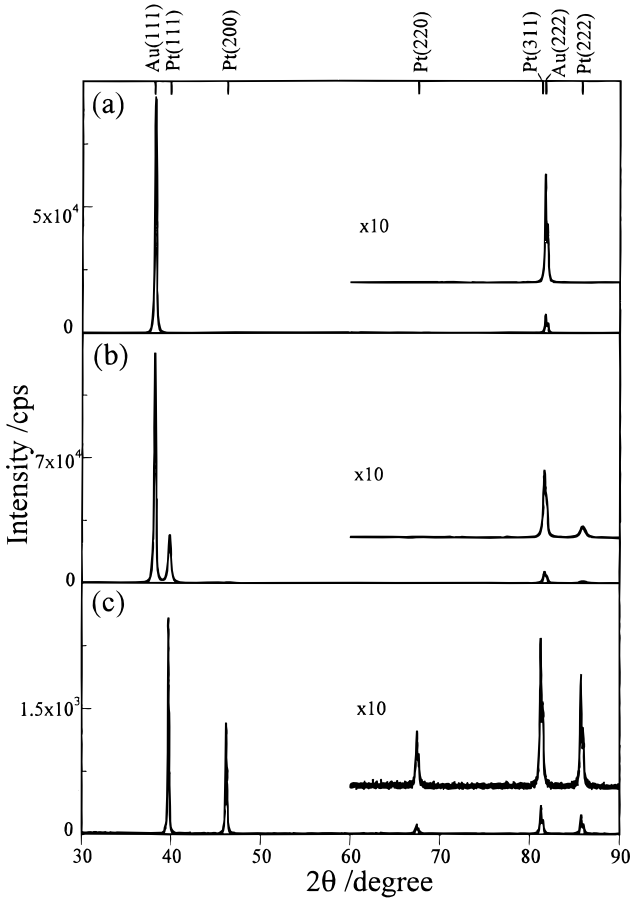

Figure 6. XRD patterns of (a) a gold electrode evaporated on a glass slide at 300 °C (Au/glass slide), (b) a gold electrode evaporated on a glass slide at 300 °C followed by electrochemical deposition of platinum at 0.05 V for 45 min in a solution containing 50 mM H_2SO_4 and 1 mM H_2PtCl_6 (Pt/Au/glass slide), and (c) a bare polycrystalline Pt disk.

The reflection of gold should be attributed to the Au(111) substrate since the penetration depth of the X-ray is much deeper than the thickness of the platinum deposit layer. In the case of the polycrystalline Pt disk, the (200), (220), and (311) reflections of platinum were also observed (Figure 6c). These results clearly show that a (111) orientated platinum bulk phase was formed on the Au(111) substrate by electrochemical deposition.

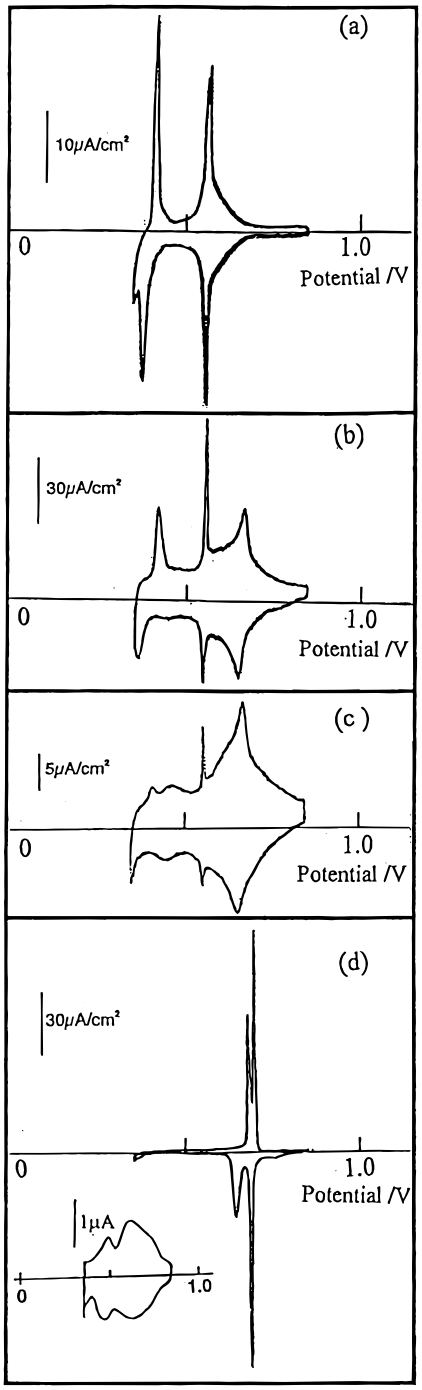

Figure 7. Cyclic voltammograms in a solution containing 50 mM H_2SO_4 and 5 mM $CuSO_4$ of (a) a bare Au(111) single-crystal electrode, (b, c) an Au(111) single-crystal electrode with an electrochemically deposited platinum layer formed in a solution containing 50 mM H_2SO_4 and 0.01 mM H_2PtCl_6 at +0.75 V for (b) 30 min and (c) 60 min, and (d) a bare Pt(111) single-crystal electrode. The inset in part d is the CV for a polycrystalline platinum electrode in the same solution. Sweep rate: 5 mV/s.

Underpotential Deposition of Copper and Hydrogen on a Platinum-Deposited Surface. Since the XRD and STM measurements provide information only about the bulk phase and of the surface but local structure, respectively, the underpotential deposition (UPD) reactions of copper and hydrogen on the electrochemically deposited platinum layer were investigated in order to examine the order of the entire surface. Electrochemical studies of gold and platinum single crystals of various surface orientation by many research groups have shown that the shape of the cyclic voltammogram (CV) for UPD reactions is very sensitive to the surface structure of the electrode.

TABLE 1: Fraction of the Free Gold Site, q_{Au}, and Deposited Platinum, q_{Pt}, on the Surface of Electrochemically Deposited Platinum on the Au(111) Electrode (See Text for Details)

			q_{Pt}	
deposition time	deposited amount	q_{Au}	Cu-UPD	H-UPD
30 min	2.1 ML	0.44	0.56	0.50
60 min	4.2 ML	0.11	0.89	0.80

Figure 7 shows CVs in a solution containing 50 mM H_2SO_4 and 5 mM $CuSO_4$ of (a) a bare Au(111) single-crystal electrode, (b, c) an Au(111) single-crystal electrode with an electrochemically deposited platinum layer formed in a solution containing 50 mM H_2SO_4 and 0.01 mM H_2PtCl_6 at +0.75 V for (b) 30 min and (c) 60 min, and (d) a bare Pt(111) single-crystal electrode. The inset of Figure 7d is a CV of a polycrystalline Pt electrode in the same solution. The deposited amount of platinum calculated from the charge passed during the deposition is equivalent to 2.1 and 4.2 monolayers for a 30 min and 60 min deposition, respectively. Two pairs of redox peaks were found at +0.41 and +0.56 V at the Au(111) single-crystal electrode (Figure 7a). Two very sharp anodic peaks at +0.67 and +0.70 V, a sharp cathodic peak at +0.68 V, and a relatively broad cathodic peak at +0.64 V were observed at the Pt(111) single-crystal electrode (Figure 7d). The CVs observed at the Au(111) and Pt(111) electrodes are in good agreement with those previously reported.[1−4] At the Au(111) electrode on which platinum was deposited for 30 min (Figure 7b), a new peak at +0.67 V with a shoulder around +0.65 V was observed in addition to the two peaks observed at the Au(111) electrode. The peak position of the former peak, +0.67 V, is close to those of two peaks observed at the Pt(111) electrode. The former and the latter peaks became larger and smaller, respectively, as the deposition time was increased to 60 min (Figure 7c). Thus, the peaks at +0.56 and +0.41 V observed in Figure 7b,c are due to the UPD of copper on the uncovered gold surface of the platinum-deposited Au(111) surface and the peak at +0.67 V with a shoulder at +0.65 V should be related to the UPD on the deposited Pt sites.

One can calculate the areas of the uncovered Au(111) surface and the Pt(111) surface from the integrated charges of the peaks at +0.41 and +0.56 V and of the peak at +0.67 V with a shoulder at +0.65 V, respectively. These results are summarized in Table 1. One must note that although more than a monolayer of Pt was deposited, uncovered gold areas still existed. This means the deposition was not perfectly two-dimensional.

The relatively good agreement in the peak positions of the redox peaks at the Pt(111) electrode and at the Pt-covered Au(111) electrode and the fact that only small broad peaks were observed in the CV of the polycrystalline platinum electrode for the copper UPD under the same conditions (inset of Figure 7d) suggest that the surface of the deposited platinum layer was highly ordered with a (111)-(1×1) structure. This is in agreement with the results of the *in situ* STM observations and XRD measurements described above. A relatively small (111) domain size and higher step density may be responsible for the differences in the shape and position of the redox peaks for the UPD of copper on the platinum-deposited Au(111) surface and on the Pt(111) single-crystal electrode.

Adsorption and desorption of hydrogen on the electrodes were also examined in the 50 mM H_2SO_4 solution to characterize the surface order. Figure 8a shows a CV at a single-crystalline Au(111) electrode on which platinum was deposited at +0.75

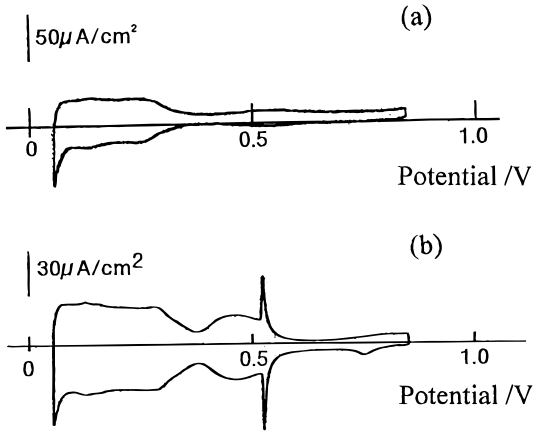

Figure 8. Cyclic voltammograms in a 50 mM H_2SO_4 solution of (a) an Au(111) electrode on which platinum was deposited at +0.75 V for 30 min in a solution containing 50 mM H_2SO_4 and 0.01 mM H_2PtCl_6 and (b) a bare Pt(111) single-crystal electrode. Sweep rate: 50 mV/s.

V for 30 min in a solution containing 50 mM H_2SO_4 and 0.01 mM H_2PtCl_6 (2.1 monolayer Pt). A square-shaped redox wave was observed in the potential region between +0.05 and +0.35 V. No peaks were found in this potential region at the bare Au(111) electrode in the same solution, and the redox wave is attributed to the UPD of hydrogen on the platinum electrode, demonstrating that the platinum was certainly deposited on the Au(111) surface. The coverage of platinum atoms estimated from the hydrogen desorption wave was 0.50, which is in good agreement with the value estimated from the UPD peaks of copper (0.56, Table 1). The number determined by the hydrogen UPD wave should be, however, more accurate because the estimation of the surface area of gold and platinum from the UPD peaks of copper are rather difficult because peaks for the copper UPD of the Au(111) and Pt(111) electrodes overlap each other.

The shape of the CV is quite different from that of a polycrystalline platinum electrode where two hydrogen adsorption/desorption peaks are observed at +0.27 and +0.13 V in the same solution. A square-shaped hydrogen adsorption/desorption wave is known to be unique for the Pt(111) phase. Figure 8b shows a CV of the Pt(111) single-crystal electrode in 50 mM H_2SO_4 solution. A square-shaped redox wave and a sharp spike at +0.53 V were observed.[28] Thus, the shape of the CV observed at the Pt-deposited Au(111) surface is the same as that of the Pt(111) single-crystal electrode except for the sharp spike. The present results suggest that the surface structure of the electrochemically deposited platinum layer on the Au(111) substrate was quite different from that of the polycrystalline platinum electrode but somewhat similar to that of the Pt(111) single-crystal electrode, confirming the conclusion drawn from results of the copper UPD. The lack of the sharp spike at the deposited platinum surface means that the surface is not perfectly (111) oriented. It was reported that the spike can be observed only when the domain of the (111) terrace exceeds a certain size.[39−41] This result is also in agreement with the results of copper UPD and those of STM measurements (Figure 3) in which smaller flat terrace domains were observed on the surface of deposited platinum compared to that of the Au(111) electrode.

As described above, although it is not an ideal layer-by-layer growth process, present results suggest a quasi-two-dimensional layer-by-layer deposition process for the electrochemical deposition of platinum.[42,43]

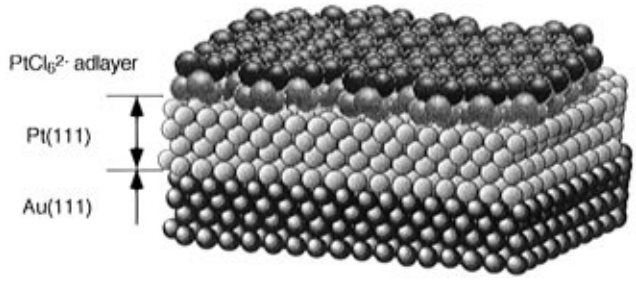

Figure 9. Schematic model for the adlayer structure of $PtCl_6^{2-}$ species adsorbed on a Pt(111) phase that is electrochemically deposited on an Au(111) substrate.

Conclusion

STM and EQCM investigations showed that the electrochemical deposition of platinum on an Au(111) electrode in acidic solutions containing H_2PtCl_6 seemed to proceed with a quasi-two-dimensional layer-by-layer growth process.[39,40] An ordered adlayer with a $\sqrt{7}\times\sqrt{7}R19.1°$ structure attributed to the weakly adsorbed $PtCl_6^{2-}$ species was observed on the electrode surface by STM measurement at a potential during electrochemical deposition of platinum. This structure disappeared if the electrode was rinsed with H_2PtCl_6-free solution and a new well-defined surface structure of Pt(111)-(1×1) was observed. Formations of the Pt(111) bulk phase and surface structure of Pt(111)-(1×1) were confirmed by XRD measurement and the UPD reactions of copper and hydrogen, respectively. Figure 9 is a schematic view of the structure of the $PtCl_6^{2-}$/Pt(111)/Au(111) system. As the $PtCl_6^{2-}$ complex is electrochemically reduced to platinum metal, the epitaxially grown Pt(111) phase is formed on the Au(111) surface and the outermost surface is always covered with the weakly adsorbed $PtCl_6^{2-}$ complex. We must note here that ca. 3% lattice mismatch between the unit lattice of Au(111) (0.288 nm) and that of Pt(111) (0.277 nm) is expected. Although it is very interesting to investigate the relaxation process during the electrochemical deposition process of platinum on Au(111), the difference between two lattice constants is too small to be investigated by the STM measurement. A more detailed investigation by grazing incident surface X-ray diffraction (GISXRD) measurement as well as of the electrochemical epitaxial growth of other noble metals is in progress.

Acknowledgment. This work was partially supported by a Grant-in-Aid for Scientific Research on Priority Area of "Electrochemistry of Ordered Interfaces" (No. 09237101) from the Ministry of Education, Science, Sports and Culture, Japan, and by the Kato Science Foundation. We are grateful to Prof. K. Shimazu for help with the XPS measurements.

References and Notes

(1) Magnussen, O. M.; Hotlos, J.; Nichols, R. J.; Kolb, D. M.; Behm, R. J. *Phys. Rev. Lett.* **1990**, *64*, 2929.
(2) Manne, S.; Hansma, P. K.; Massie, J.; Elings, V. B.; Gewirth, A. A. *Science* **1991**, *251*, 183.
(3) Hachiya, T.; Honbo, H.; Itaya, K. *J. Electroanal. Chem.* **1991**, *315*, 275.
(4) Sashikata, K.; Furuya, N.; Itaya, K. *J. Electroanal. Chem.* **1991**, *316*, 361.
(5) Kimizuka, N.; Itaya, K. *Faraday Discuss.* **1992**, *94*, 117.
(6) Chen, C. H.; Vesecky, S. M.; Gewirth, A. A. *J. Am. Chem. Soc.* **1992**, *114*, 451.
(7) Corcoran, S. G.; Chakarova, G. S.; Sieradzki, K. *Phys. Rev. Lett.* **1993**, *71*, 1585.
(8) Ogaki, K.; Itaya, K. *Electrochim. Acta* **1995**, *40*, 1245.
(9) Ikemiya, N.; Yamada, K.; Hara, S. *J. Vac. Sci. Technol. B* **1996**, *14*, 1369.

(10) Tao, N. J.; Pan, J.; Li, Y.; Oden, P. I.; DeRose, J. A.; Lindsay, S. M. *Surf. Sci. Lett*. **1992**, *271*, L338.
(11) Somoriai, G. A. *Chemistry in Two Dimensions: Surfaces;* Cornell University Press: Ithaca, London, 1981.
(12) *The Science of Noble Metal*; Tanaka, S., Ed.; Tanaka Noble Metal Co.: Japan, 1985; Vols. 1-3.
(13) Rand, D. A. J.; Woods, R. *J. Electroanal. Chem.* **1973**, *44*, 83.
(14) Furuya, N.; Motoo, S. *J. Electroanal. Chem.* **1978,** *88*, 151.
(15) Leung L. H.; Weaver, M. J. *J. Am. Chem. Soc.* **1987**, *109*, 5113.
(16) Kunkel, R.; Poelsema, B.; Verheij, L. K.; Comsa, G. *Phys. Rev. Lett.* **1990**, *65*, 733.
(17) Farrow, R. F. C; Harp, G. R.; Marks, R. F.; Rebedeau, T. A.; Toney, M. F.; Weller, D.; Parkin, S. S. P. *J. Cryst. Growth* **1993**, *133*, 47.
(18) Minvielle, T. J.; White, R. L.; Hildner, M. L.; Wilson, R. J. *Surf. Sci*. **1996**, *366*, L755.
(19) Sumino, M. P.; Shibata, S. *J. Electroanal. Chem.* **1992**, *322*, 391.
(20) Sumino, M. P.; Shibata, S. *J. Electroanal. Chem.* **1992**, *336*, 329.
(21) Goldberg, R. N.; Hepler, L. G. *Chem. Rev.* **1968**, *68*, 229.
(22) Davidson, C. M.; Jameson, R. F. *Trans. Faraday Soc*. **1965**, *61*, 2462.
(23) Ginstrup, O.; Leden, I. *Acta Chem. Scand.* **1967**, *21*, 2689.
(24) Ginstrup, O.; Leden, I. *Acta Chem. Scand.* **1968**, *22*, 1163.
(25) Ginstrup, O. *Acta Chem. Scand.* **1972**, *26*, 1527.
(26) Yamamoto, H.; Takeshi, T. *Denki Kagaku* **1961**, *29*, 396.
(27) Yamamoto, H.; Tanaka, S.; Takashi, N.; Takeshi, T. *Denki Kagaku* **1964**, *32*, 43.
(28) Clavilier, J.; Faure, R.; Guinet, G.; Durand, R. *J. Electroanal. Chem.* **1980**, *107*, 205.
(29) Zei, M. S.; Nakai, Y.; Lehmpfuhl, G.; Kolb, D. M. *J. Electroanal. Chem.* **1983**, *150*, 201.
(30) Uosaki, K.; Ye, S.; Kondo, T. *J. Phys. Chem*. **1995**, *99*, 14117.
(31) Sauerbrey, G. Z. *Z. Phys.* **1959**, *155*, 206.
(32) Buttry, D. A.; Ward, M. D. *Chem. Rev.* **1992**, *92*, 1355.
(33) Shimazu, K.; Yagi, I.; Sato, Y.; Uosaki, K. *Langmuir* **1992**, *8*, 1385.
(34) Uosaki, K.; Ye, S.; Oda, Y.; Haba, T.; Hamada, K. *Langmuir* **1997**, *13*, 594.
(35) *Handbook of Chemistry and Physics*, 70th ed.; CRC Press: Boca Raton, 1990; p F54.
(36) Bassett, D. W.; Webber, P. R. *Surf. Sci.* **1978**, *70*, 520.
(37) Wagner, C. D.; Riggs, W. D.; Davis, L. E.; Moulder, J. F.; Muileuberg, G. E. H*andbook of X-ray Photoelectron Spectroscopy*; Perkin-Elmer Corp.: Eden Prairie, 1979.
(38) JCPDS card of No. 4-0784 and 4-0802: Swanson, H. E.; Tatge, E. *JC Fel. Rep., NBS*, **1950**.
(39) Clavilier, J.; Achi, K.; Rodes, A. *Chem. Phys.* **1990**, *141*, 1.
(40) Motoo, S.; Furuya, N. *Ber. Busen-Ges. Phys. Chem.* **1987**, *91*, 457.
(41) Kita, H.; Ye, S.; Aramata, A.; Furuya, N. *J. Electroanal. Chem.* **1992**, *295*, 317.
(42) Purcell, S. T.; Arrott, A. S.; Heinrich, B. *J. Vac. Sci. Technol. B* **1988**, *6*, 794.
(43) Egelhoff, W. F., Jr.; Jacob, I. *Phys. Rev. Lett.* **1989**, *62*, 921.